Carpathian Journal of Earth and Environmental Sciences, February 2017, Vol. 12, No. 1, p. 207 - 224

SYSTEMATIC DIGITAL TERRAIN MODEL CONSTRUCTION AND MODEL VERIFICATION WITH MULTI-SOURCE FIELD DATA. MORPHOTECTONIC ANALYSIS IN THE VILLANY HILLS AND ITS SURROUNDINGS, SW HUNGARY

Attila PETRIK[1] & Gyozo JORDAN[2]

[1]Department of Physical and Applied Geology, Eötvös University, Pázmány Péter sétány 1/C, 1117, Budapest, Hungary, petrik.atus@gmail.com

[2]Department of Chemsitry, Szent István University, Práter Károly u.1., 2100, Gödöllő, Hungary, gyozo.jordan@gmail.com

Abstract: The objective of this study is presenting a systematic digital terrain modelling method and testing its capabilities on poorly defined thrust fault-related actively uplifting area. A further objective is to present a detailed verification of digital terrain modelling results using field observation of more than 1,000 structural field measurements, geophysical seismic sections and geological information. Finally, tectonic stress field models are compared to the terrain modelling results and relating digitally identified geomorphological features. Systematic digital terrain modelling proceeds from simple univariate analysis of elevation and its derivatives to the more complex bivariate stereonet analysis, digital drainage network analysis and to lineament pattern analysis. Morphotectonic lineaments identified on shaded relief map were used to compare them to the known tectonic lines in the study area. The combined usage of 200 digital morphologic cross-sections and slope-breaks on profile curvature maps were used to reveal the asymmetry of surface topography along the known tectonic lines. Linear valleys and ridge lines were defined as drainage and watershed lines by means of digital drainage network analysis. Results show that the orientation of the measured structural field data correlate to the orientation of the various observed morphological lineaments such as drainage elements. This study identified valley rotation and en-echelon arrangement of some morphological features in the study area, together with a major strike-slip fault delineating the southern boundary of the studied thrust zone, unknown before.

Keyword: DEM analysis, digital geomorphometry, morphotectonics, geological field verification, image processing

1. INTRODUCTION

Digital elevation models (DEMs) provide an opportunity to quantify land surface geometry in terms of elevation and its derivatives. Morphological analysis of topographic features has long been applied in structural and tectonic studies (Frisch, 1997; Hobbs, 1912; Siart et al., 2009; Wu et al., 1993) and has become a fundamental tool in tectonic analyses (Cotilla et al., 2007; Drury, 1987; Gillespie, 1980; Parul et al., 2013; Ruibo & Weiming, 2009; Salvi, 1995). Although the interpretation of land morphology in terms of geological structures is well-established (Burbank & Anderson, 2001; Keller & Pinter; 1996; Prost, 1994) there are few case studies documented in the literature involving the consistent application of available digital terrain analysis methods for tectonic geomorphology (Jordan, 2003; Jordan et al., 2005). Most of the tectonic studies applying digital terrain models use shaded relief models either alone (Byrd et al., 1994; Collet et al., 2000; Simpson & Anders; 1992) or in combination with remotely sensed images on a regional scale (Chorowicz et al., 1999; Florinsky, 1998; Grohmann et al., 2007). Digital tectonic geomorphology is the integration of three components: structural geology, geomorphology and digital terrain analysis (DTA) (Jordan & Csillag, 2003). From the tectonic geomorphological point of view, the identification of thrust faults is one of the most challenging tasks

because most of them intersect the Earth's surface at very low angle (Burbank & Anderson, 2001; Ramsay & Huber, 1987). In comparison to normal and strike-slip faults, fewer ground ruptures resulting from thrust faults have been studied in detail. In our study area there are several thrusts faults and fold-systems providing a challenge for unveiling the impacts of complex tectonics on surface morphology.

The objective of this study is presenting a systematic digital terrain modelling method (Jordan et al., 2005) and testing its capabilities on poorly defined thrust fault-related actively uplifting area. The analysis proceeded from simple univariate elevation studies, through differential geometric surface analysis and drainage network analysis, to the multivariate interpretation of results using GIS technology. A further objective is to present a unique detailed verification of digital terrain modelling results using field observation of more than 1,000 structural field measurements, geophysical seismic sections and geological information. Similar detailed terrain modelling verification is poor in literature. Finally, tectonic stress field models are compared to the terrain model results and relating digitally identified geomorphological features.

2. STUDY AREA

The investigated area is located in the south-western part of the Pannonian Basin, where moderately elevated hills (300-400 m) comprising Mesozoic sedimentary rocks rise above the lowlands of young Tertiary rocks in the south (Fig. 1a).

The Villany Hills, Hungary, within the tectonic Tisza Unit are made up by NW vergent Mesozoic nappes including Variscan crystalline basement, Late Paleozoic, post-Hercynian cover with siliciclastic rocks and Mesozoic carbonates (Nagy & Nagy, 1976; Vadász, 1935) (Fig. 1a,b). The beginning of Late Cretaceous nappes formation can be related to the development of the flexural basin that came into existence already in the Upper Cretaceous (Albian–Cenomanian stage) (Császár, 2002). Paleogene and Early-Middle Miocene sediments are thin or completely missing, only preserved in local basins. The whole area is generally covered by transgressive clastic Late Miocene, known as Pannonian deposits (Kleb, 1973). These lake-delta and alluvial beds partly cover; partly surround the present elevations (Fig.1a).

The study area, a part of the former European Tethyan margin, suffered a very complicated Tertiary tectonic history, dominated by transpression (Csontos et al., 2002). Several structural phases have been identified in the wider study area based on paleostress and seismic data (Benkovics, 1997; Petrik, 2009). Most of them show shortening and strike-slip deformations creating high amplitude folds and thrust faults.

The Villany Hills and its surroundings can be divided into four sub-areas based on Bouguer gravitational anomalies, geomorphological and geological considerations (Fig. 1a). These are (1) the Villany Hills, (2) the relatively flat area of the Drava Basin in the south, (3) the Karasica area in the east and (4) the Baranya Hills in the north (Fig.1a). The Drava Basin was excluded from further analysis in this study because the contour line-based DEM's vertical resolution is too large and the flat basin area does not represent terrain features but systematic errors along contour lines.

Elevations in the study area range between 82 m a.s.l. in the Drava Basin and 435 m a.s.l. in the Villany Hills, with an average elevation of 251 m a.s.l. In the Villany Hills a dozen of ENE-WSW and NE-SW trending deeply incised valleys are prevailing whose orientation is slightly changing from east to west (Fig. 2). These valleys are subparallel to the major thrust faults of the area (Fig. 2). Some valleys have zig-zagged/rectangular shape at the northern margin of the Villany Hills. Subparallel N-S and NNW-SSE trending straight and slightly curving 5-15 km long valleys predominate in the Baranya Hills (Fig. 2). Most of them are changing their orientation and turning away in front of the uplifted northern flank of the Villany Hills. NNE-SSW and NE-SW tributaries are predominant along the main NNW-SSW trending long valleys in the northern part of the Baranya Hills while in the south they are scarce (Fig. 2). In the northwestern part of the Baranya Hills some deeply incised N-S oriented short valleys can be seen in an uplifting area where the majority of them are not completely connecting to the long (~5-15 km) N-S oriented valleys located south of them (Fig. 2). In the Karasica area some NW-SE trending zig-zagged shape valleys are observable on shaded relief model (Fig. 2).

The Villany Hills and the surroundings are uplifting while the Drava Basin is subsiding in the Carpathian Basin at present proven by geophysical and geodetical data (Bada et al., 2007; Grenerczy & Bada, 2005).

3. MATERIALS AND METHODS

3.1 Geometric and spatial analysis of morphological features associated with fractures and thrust faults

In this study the DEM of the Villany Hills was obtained from the national military DTA-50 digital grid elevation database, initially produced via a third-order spline function to interpolate from the

original data set of 10 m contour lines. The histogram of grid elevations shows systematic error in the DEM as spikes corresponding to the original contour lines at 10 m intervals (Jordan, 2003). The horizontal resolution of the grid is 50x50 m and the vertical resolution is 1 m. Elevations above sea level are given as integers in metres.

Structural discontinuities in rocks most often result in linear morphological features along the intersection of fracture plane and land surface. Linear morphological expressions of fractures include: (1) linear valleys, (2) linear ridgelines and (3) linear slope-breaks that can be identified as lineaments in remotely sensed images or digital elevation models (DEMs). The main geometric characteristics of a single linear line are orientation and length (continuity) and in case of curved line, curvature (Jordan et al., 2005).

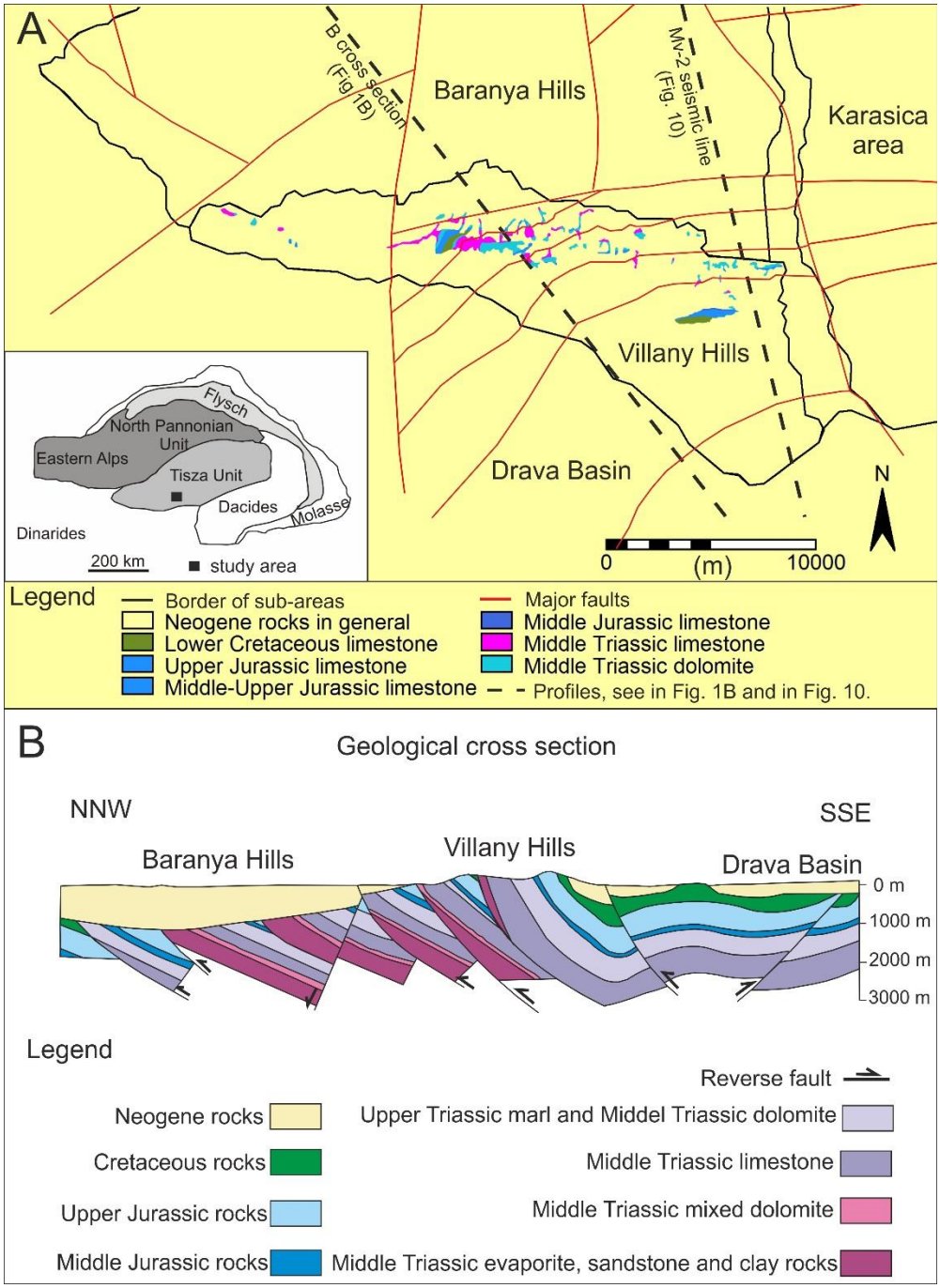

Figure 1.a. 1: 100 000 geological map of the studied area with major tectonic lines (Gyalog & Síkhegyi, 2010) and the borders of the delineated sub-areas. Note the Mesozoic rocks in the Villany Hills and the dominance of Neogene rocks in the surrounding area. Figure 1.b**.** Modified and redrawn NNW-SSE geological cross-section across the Villany Hills after (Rakusz & Strausz, 1953). The trace of the section is on Figure 1a.

Linear fracture traces are most obvious in the case of high-dip faults of normal, reverse and strike-slip type while thrust faults tend to appear irregular in topography (Drury, 1987; Goldsworthy & Jackson, 2000; Prost, 1994).

In the studied area numerous NE-SW trending thrust faults can be found resulting in a very complex structure associated with different fold systems. Reverse and thrust faults are the most difficult to identify because thrusts usually cut a land surface at about 30º angle but, in fact, thrusts and reverse faults can cut the surface at any angle and may occasionally be overturned at the surface (Keller & Pinter, 1996). Due to the low-angle intersection of thrust faults with the earth's surface, the traces of thrusts are often affected by topography and can be highly sinuous, rendering it more difficult to identify as a linear feature (Jordan, 2003). The assemblage of landforms associated with reverse or thrust faulting include steep mountain fronts, fault scarps, extensional features, landslides and different fold systems (Burbank & Anderson, 2001; Keller & Pinter, 1996). Thrust faults are often accompanied by normal faults with strike oblique to the main shortening direction and they are typically in the hinges creating en-echelon crestal grabens and shear zones with respect to the thrust trace.

3.2 Digital feature recognition and morphometric parameter extraction from DEMs

In geomorphometric studies of landscape the five basic parameters calculated are elevation, slope, aspect, profile and tangential curvatures according to Evans' general geomorphometric method (Evans, 1980), as extended with the singular points (local minima and maxima, saddle points and flats) and flow boundaries (valley and ridge lines) by (Florinsky, 1998; Jordan, 2007; Onorati et al., 1992). In order to implement the systematic geomorphometric analysis, five major fields of terrain modelling were used for integration in this paper: (1) elevation analysis, (2) numerical differential geometry, (3) digital drainage network analysis, (4) digital geomorphometry, and (5) multivariate analysis with GIS, according to (Jordan et al., 2005).

Systematic digital terrain modelling proceeds from simple univariate analysis of elevation and its derivatives to the more complex bivariate stereonet analyses, digital drainage network analysis and lineament pattern analysis, to the multivariate interpretation of results using GIS technology. At each step, digital image processing such as histogram analysis and spatial filtering is applied to the calculated terrain models such as slope, relief and curvature maps.

3.3 Analysis of elevation data

In terms of elevation analysis, the shaded relief model was a key component throughout this study because it was the most suitable terrain model for the recognition and interpretation of complex morphological features related to the thrust zones. Eight shaded relief models were calculated at an azimuth interval of 45° and constant insolation inclination of 45°. The models used Lambertian reflection method and six-time vertical exaggeration. Since locations of shadow contrast change with illumination, azimuth and inclination, lineament identification was enhanced by the overlay of elevation contour map. Lineaments were drawn on-screen by hand in shaded relief models and then the resulting eight lineament maps were combined into one by eliminating duplicate lines in the digital overlay. The orientation of the obtained lineaments was compared to the regional tectonic lines by overlying the features to check the geometrical coincidence.

The length azimuth rose diagram was calculated for the lineament map derived from the DEM smoothed with a 550 x 550 m moving average filter to suppress small elements and to enhance large-scale significant features in the study area (see Fig. 7). Several window-sizes were tested for moving average smooth to find the best compromise between noise removal and keeping information detail.

Lineament density map was also created for increasing aggregation cell sizes from 50 x 50m to 5,000 x 5,000 m. The 500 x 500 m pixel size proved to be the most informative for morphotectonic interpretation (e.g. Fig. 7). The thus obtained density map was smoothed using a simple moving average smooth at the end to increase visual interpretability.

More than 200 digital cross-sections were made across the Villany Hills and Baranya Hills mainly in perpendicular directions to the principal morphological features and the known tectonic lines in order to study the local conditions at prominent features (e.g. Fig. 2a). The difference between the highest point and the lowest point divided by the median elevation value in a moving window was used to calculate the relief map.

The window size was increased from 100 metres to 10,000 metres (ca. one quarter of the study area) and the final window size was defined by visual inspection when the most distinct homogeneous areas resulted (see Fig. 3a).

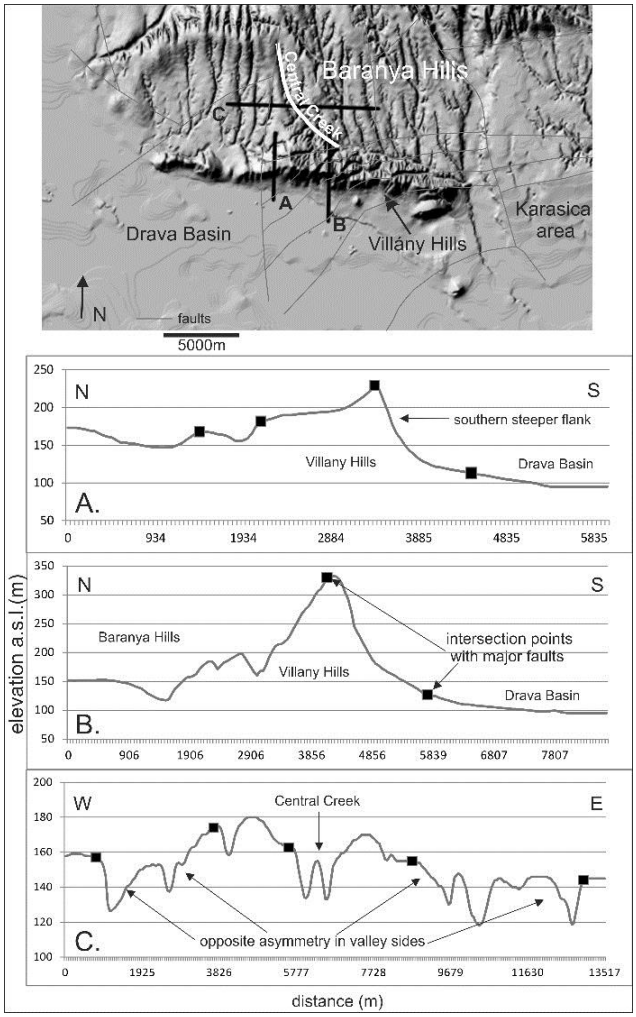

Figure 2. Some digital morphological cross-sections across the Villány Hills. The black squares in the cross-sections indicate the intersection points with tectonic lines taken from (Gyalog & Síkhegyi, 2010). Grey-scale shaded relief model is also shown for orientation.

3.4 Numerical differential geometry calculations

Terrain slope and aspect calculations used the unweighted eight-point numerical differentiation method (Prewitt operators) for its smoothing effect. Slope and aspect values are given as integers in this study. Lines of abrupt slope-breaks represented by the profile curvature map were located by the identification of the highest curvature values in the histogram. According to Evans (1972), the statistical properties of point attributes are more stable if the DEM is smoothed before analysis. Based on these results, the original DEM of the study area was smoothed with 150x150m moving average filter prior to curvature calculations. Filter kernel size for smoothing was selected on the basis of the scale of the feature to be studied and the characteristics of the filter applied. In the case of curvatures using second derivatives that strongly increase relative error (Florinsky, 1998), the 150x150m kernel size seemed the best compromise between error reduction and feature (slope-break) recognition based on visual inspection of the curvature maps using increasing smoothing kernel sizes.

In order to improve classification of aspect data based on their histograms, the aspect histogram curves were smoothed with a five-point median filter [44] to remove the systematic error shown as pikes in at values of 45° azimuth due to numerical derivation over a rectangular grid [14]. Aspect rose diagrams discussed in this paper (see Fig. 4b) are based on the smoothed histograms. In order to capture areas of uniform aspect value the aspect map was post-processed with a 500x500m majority filter (see Fig. 4c). Aspect data was displayed as frequency histograms and rose diagrams.

Histogram peaks were sliced and displayed as homogeneous areas of elevation, aspect and slope classes in different colours.

Slopes with more than 1° and aspect data were also used to derive stereograms on the Schmidt hemisphere with upper projection. We aim to see if steep slopes are associated with preferential aspect directions. Uniform aspect with steep slopes may indicate tectonic origin in an area (Jordan, 2003). If these areas are located along major lineaments, the tectonic origin is further indicated. It is noted, however, that the effects of secondary processes such as lithological control, wind or gully erosion can also result in morphological features similar to morphotectonic landforms. This confirms the need for thorough field observation and verification as demonstrated in this study.

The localization of surface-specific points, i.e. local maxima (peaks), minima (pits), saddle points (passes), flats and slope-breaks is fundamental in digital geomorphologic analysis (Peucker & Douglas, 1975; Takahashi et al., 1995). Peaks and pits were calculated using simple ‘higher than’ algorithms (Garbrecht & Martz, 1999). Artificial flat areas in the DEM were filtered out by the identification of flat areas defined as pixels with no runoff. In this study, the gradient (slope and aspect) and curvatures were calculated for regular points only having defined gradient, while inflex points were not considered for morphotectonic interpretation.

3.5. Digital drainage network extraction

Whipple & Tucker (1999) elaborated standard channel network analysis based on stream power rule and long profile development. Instead of valley

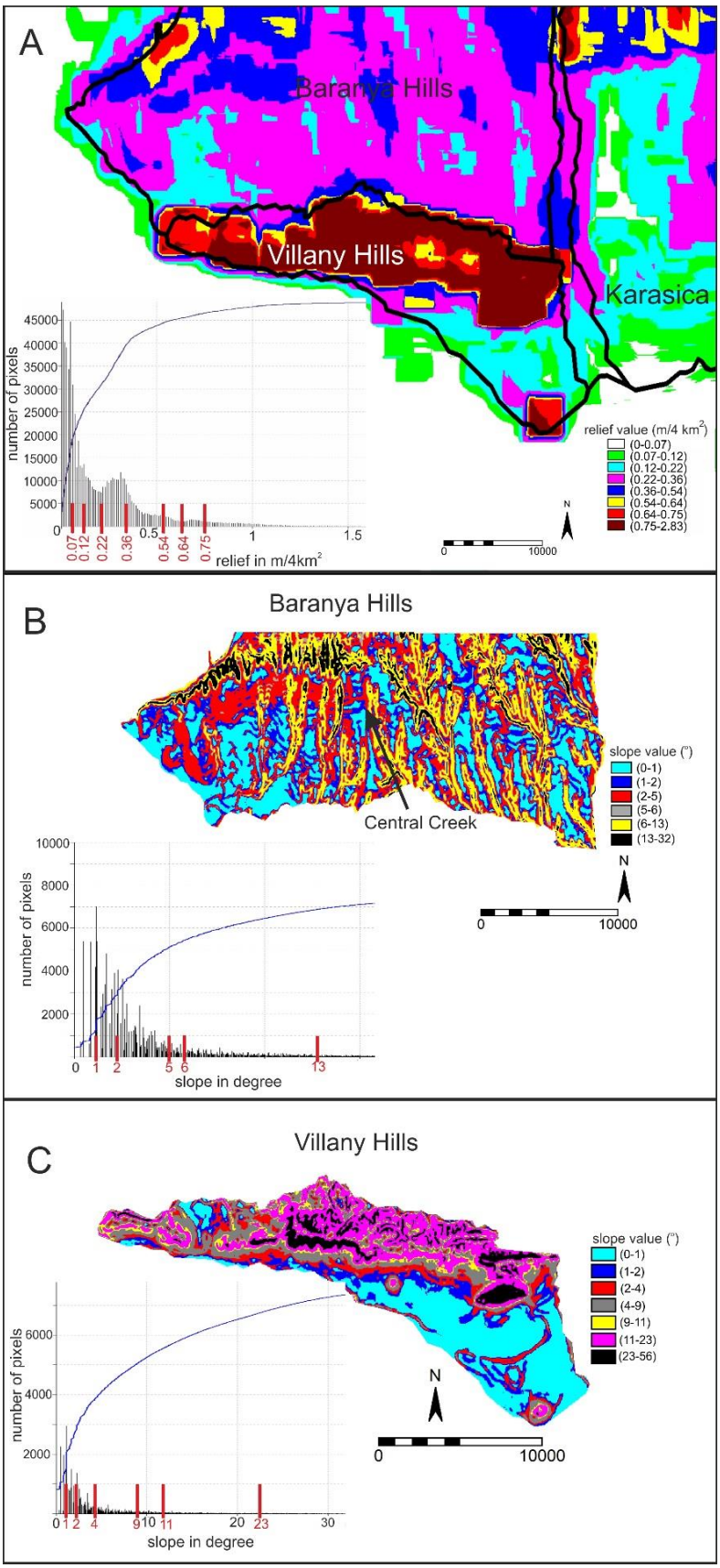

Figure 3 a. The classified relief map for the total area. Figure 3 b. The classified slope map for the Baranya Hills and Figure 3 c. Villány Hills. Slope values are displayed in degrees. Insets show corresponding histograms. Colour codes (thick red lines on histogram axes) are identical with classes defined by histogram slicing technique. See text for details.

development modelling, the objective of this study is the accurate geometric identification of valleys and ridge lines only as drainage channels and watershed divides, respectively. The drainage network extraction based on D8 method (Douglas, 1986) in this study was carried out with the TOPAZ model developed by Martz & Garbrecht (1992). The network identified with this method provided fully connected, convergent and unidirectional down-slope channel network. Accordingly, the drainage lines are defined as the cells that have an upstream drainage area larger than a user-defined threshold drainage area, the critical source area (CSA). The selection of an adequate threshold is crucial, because it defines the dimensions of the valleys to be analysed in the studied terrain. A CSA of 100 ha yielded high density and single pixel drainage network in this study. The orientation of drainage lines were calculated after smoothing the vectorised channel lines with a 1,000m width tunneling operation. This operation examines every three consecutive points within a line and omits the middle point if it falls outside the user-defined tunnel-width.

3.6 Digital geomorphometry and field verification

For morphotectonic interpretation upper hemisphere Schmidt stereograms with contour lines were constructed using integrated step function of the Rockworks© 15 software (see Fig. 5) for slope > 1º in order to see if steep slopes tend to face in the same direction along major lineaments. If so, it may indicate tectonic origin. Profile curvature, aspect, and slope conditions were examined in a 500 m buffer zone along the main known tectonic lines to see if steep slopes, slope-breaks and uniform hillsides are associated with these lines.

Finally, detailed verification of DTA results was carried out and all the terrain analysis results including lineament statistics were compared to field observations at points and to geophysical 2D reflection seismic profiles and geological maps using GIS overlay. Structural measurements were carried out in different aged rocks (Triassic, Jurassic, Cretaceous, Late Miocene and Pleistocene) and at various morphological settings such as valleys, hillsides and quarries covering the whole studied area. We focused on measuring brittle structural elements (faults with striae and joints). More than 1,000 structural data were measured and integrated into a database as ground truthing in order to verify the existence of lineaments derived from the systematic DTA as true rock fractures. The field data was also used to determine the paleo-stress field and structural evolution of the studied area. The separation and classification of stress fields were based on relative chronology between structures, the position of main stress axis and the similar extensional and compressional direction. Then stress fields were integrated into main structural phases where the youngest one (from Pliocene to date) received particular attention in this paper due to its possible influence on the evolution of morphological features. The structural field data and the youngest structural phase (neotectonic phase?) were compared to the terrain modelling results in order to examine the relationship in the orientation of identified lineaments and observed fault zones. In this way we were able to give a possible kinematics to the extracted lineaments (valleys/ridges/slope-breaks) and determine the stress field under which they might have evolved.

2D reflection seismic profiles were also involved to examine the relationship between surface topography and subsurface structures. It is believed that in this way the most thoroughly verified morphotectonic model has been achieved.

4. RESULTS

4.1. Digital terrain analysis

4.1.1. Elevation data analysis

Elevations in the study area range between 82 m a.s.l. in the Drava Basin and 435 m a.s.l. in the Villany Hills, with an average elevation of 251 m a.s.l. The Villany Hills have a strong asymmetry in topography with steeper slopes on the southerly hill slopes (Fig. 2a,b). The steeper southern flanks of the Villany Hills rise abruptly from the surrounding lowlands of the Drava Basin (Fig. 2a,b).

The NNW-SSE and N-S oriented subparallel valleys in the Baranya Hills indicate another asymmetry on the E-W oriented elevation cross-section (Fig. 2c). It can be clearly seen that the valley sides show opposite asymmetry to the west and to the east of the Central Creek which is found in the middle of the Baranya Hills (Fig. 2c). The western valley sides have steeper slope west of the Central Creek while the asymmetry is just the opposite to the east of the Central Creek (Fig. 2c).

In addition, the orientation of the long sub-parallel valleys is also slightly changing from N-S to NNW-SSE form the west to the east in the Baranya Hills. Some intersection points with tectonic lines were also displayed on cross sections where their coincidence with abrupt elevation changes are fairly well especially in the Villány Hills (Fig. 2a,b,c).

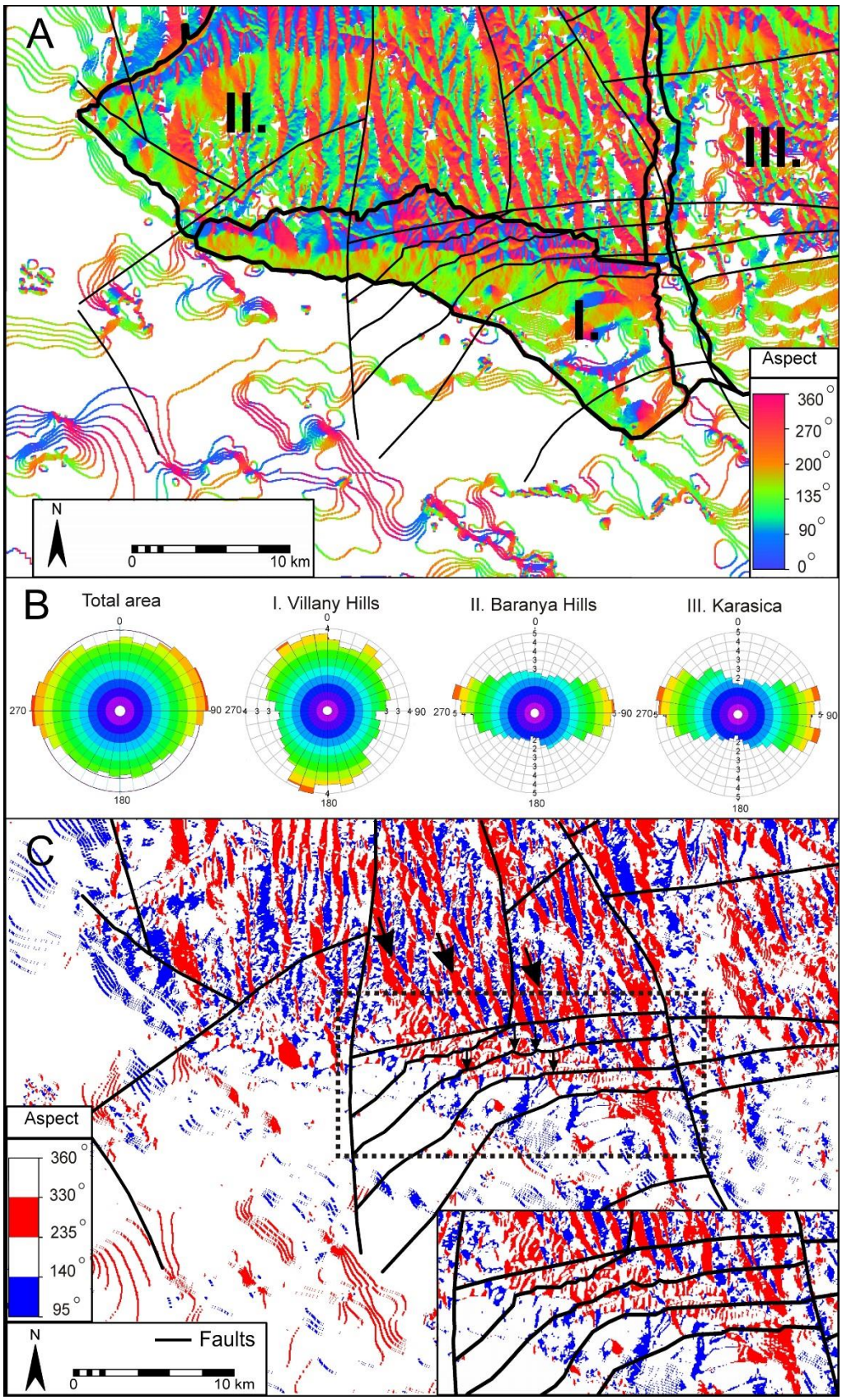

Figure 4 a. The aspect map of the study area with tectonic lines taken from (Gyalog & Síkhegyi, 2010). Roman numbers indicate the sub-areas (I. Villány Hills, II. Baranya Hills, III. Karasica). Figure 4 b. Aspect rose diagrams of total area and sub-areas. Figure 4 c. The dominant aspect directions (95-140° and 235-330°) compared to the main tectonic lines. The black arrows indicate the dominant orientation of morphological features.

The relief map calculated in 2,050 x 2,050 m window (Fig. 3a) displays the highest relief values in the Villany Hills and its surroundings (2.83 m/4 km^2). More than half of the studied area is dominantly flat and its relief value is rather low (0 – 0.12 m/4 km^2) corresponding to the extensive lowlands of the Drava Basin in the south. Relatively high relief values (0.64 – 2.83 m/4 km^2) are also experienced in the northern and southern boundaries of the E-W oriented Villany Hills. Inside the Baranya Hills the highest relief values (~0.75-2.83 m/4 km^2) can be observed at its northwestern and northeastern margins (Fig. 3a) where the lineament density is high (see Fig.7) and the valleys have relatively short and deep.

The Karasica area east of the Villany Hills can be regarded as a homogenous area with small relief values (~0.07-0.12/4 km^2).

4.1.2 Differential geometry analysis: slope, aspect and curvature maps

The steepest slope value is 56° and the average value is 2.4° for the total area. The cumulative percentage area-slope curve shows that the slopes are less than 4° in 53% of the area. Four classes of slope were identified for the total area based on the break points of the slope cumulative histogram and these are <=1°, 1-3°, 3-4° and > 4°, respectively.

Since the four sub-areas have different topography slope changes were also examined for the Baranya Hills and the Villany Hills separately (Fig. 3b,c). In the Baranya Hills six slope classes could be identified <=1°, 1-2°, 2-5°, 5-6°, 6-13° and >13° (Fig. 3b). The steepest slope value (> 13º) are observed at the northwestern and northeastern margins of the Baranya Hills similarly to highest relief values (Fig. 3a). In these area many short deeply incised N-S oriented valleys are found in an uplifted area (Fig. 3b). Areas with high slope values can also be seen along N-S and NNW-SSE oriented long valleys but they are not continuous and concentrated on certain reaches (Fig. 3b). The classified slope map enhanced excellently the almost equidistantly aligned sub-parallel valleys in the Baranya Hills.

7 slope classes were separated in the Villany Hills based on the cumulative histogram. The highest slope values in the total area can be found here (23-56°). Large continuous areas have large slope values along the southern slope of the E-W oriented Villany Hills but separate steep hillsides can be also observed in the eastern part of the hills. High slope values appear along the deeply incised NE-SW oriented valleys inside the hills (Figs. 2,3c). A significant break point in the slope cumulative histogram is at 4° capturing the regional slope-break line between the Drava Basin and the Villany Hills.

Aspect data as opposed to shaded relief model is independent of illumination parameters and, therefore, accurately locates valley lines, slope breaks and ridges. It is obvious in Fig. 4a that the major thrust faults in the Villany Hills run parallel along lines of sharp aspect changes that correspond to sharp valleys and ridge lines. The aspect rose diagram for the total area (Fig. 4b) and sub-areas reveal some differences in the orientation pattern of morphological features. In the Baranya Hills and the Karasica area two major directions are predominant: one facing SE (70-110º) and another pointing almost to the opposite direction (260-300º) (Fig. 4c). The two aspect frequency peaks correspond to the valley-sides of the NNW-SSE and N-S oriented sub-parallel valleys. In the Baranya Hills and the Karasica region the steeper slopes face to the E-W direction (Fig. 5).

The north and the south facing hillsides are prevailing in the Villany Hills due to its strike (Fig. 4b). According to figure 5, slopes facing to the N and S directions tend to be steeper in the Villany Hills. This corresponds to the E-W strike of the hills along the Mesozoic thrust faults.

The classified aspect map for the total area reveals two major aspect directions. One facing to 235-330° while the other is facing to 95-140° (Fig. 4c). Both of them correspond to the NNW-SSE to NNE-SSW trending hillsides and valleys which dominate especially in the northern and eastern part of the study area (Fig. 4c). This pattern is also present in the Villany Hills but the corresponding valleys are much shorter and are arranged in E-W zones between the thrust fault lines (Fig. 4c). These valleys are N-S orientated but their orientations differ more than 20 degrees from the orientations of the valleys in Baranya Hills and Karasica (Fig. 4c). According to figure 5, slopes facing to the N and S directions tend to be steeper in the Villany Hills. This corresponds to the E-W strike of the hills along the Mesozoic thrust faults. In the Baranya Hills and the Karasica region the steeper slopes face to the E-W direction (Fig. 5).

It is interesting that areas with uniform aspect (300-330º) and steep slope angles (>40º) have linear borders coinciding with the major thrust fault lines in the Villany Hills (Fig. 4c).

The classified profile curvature map clearly shows the slope breaks located parallel to the ridge lines in the southern flank of the Villany Hills where the highest slope values were also observed (Fig. 6).

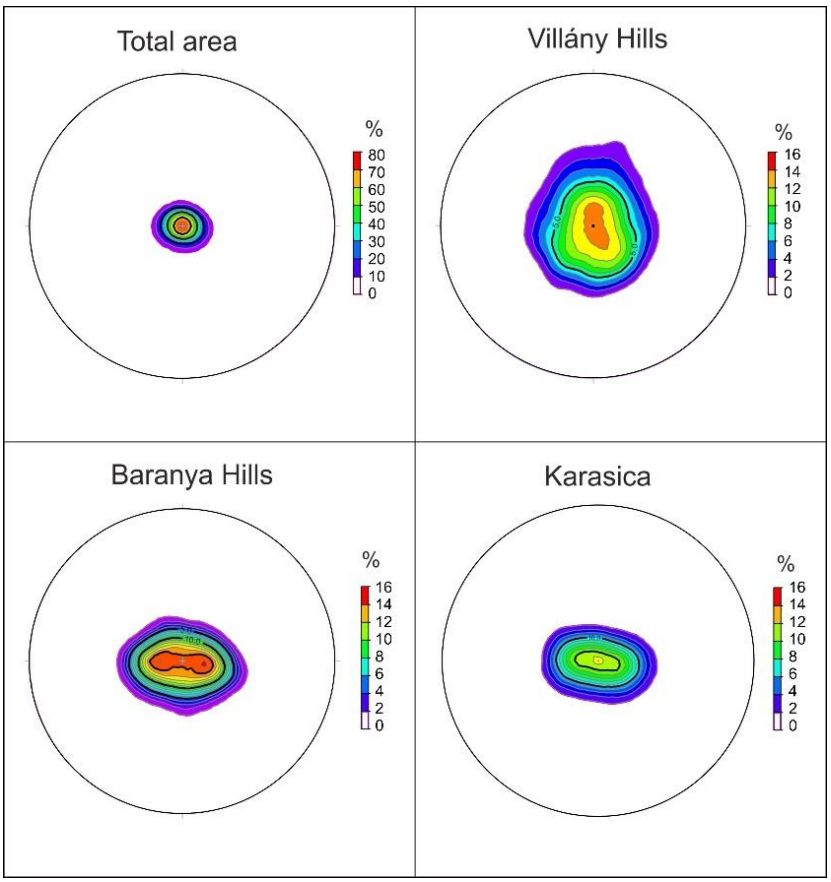

Figure 5. Stereograms on Schmidt hemisphere with upper projection constructed from the aspect and slope values (more than 1°) in each DEM cell (n = the number of data).

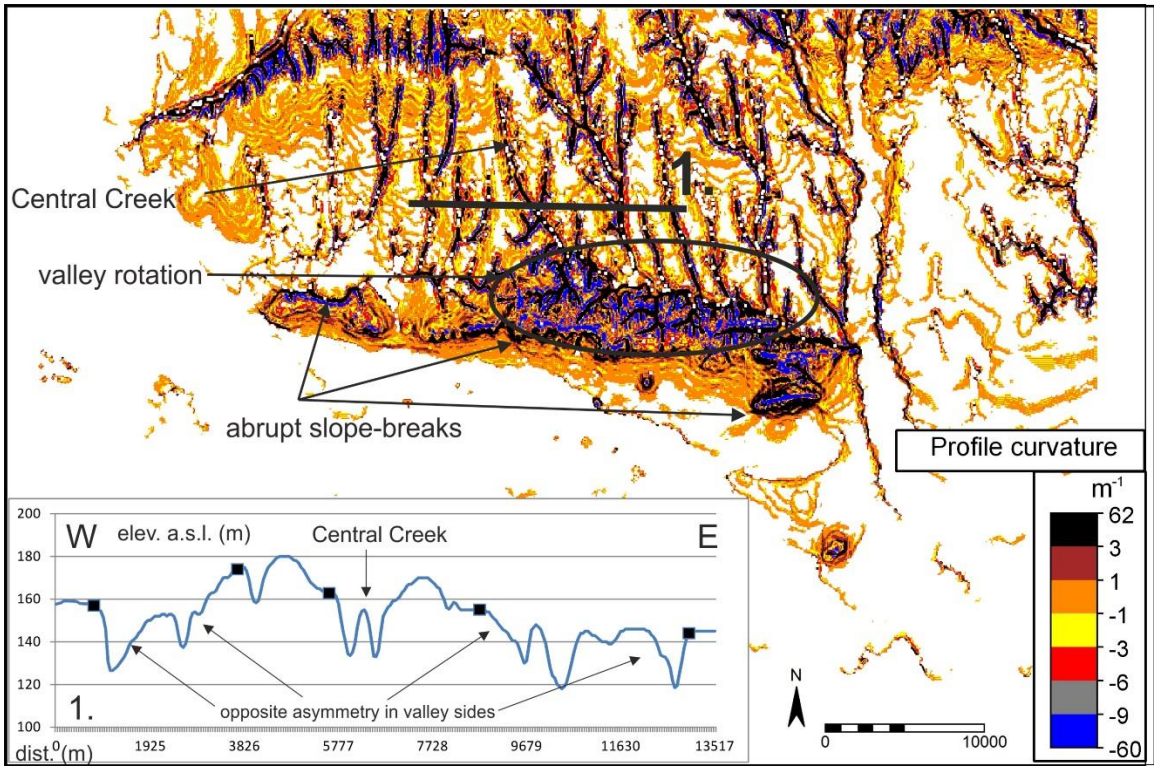

Figure 6. The classified profile curvature map of the study area. The black shading having positive values displays concave forms corresponding to valleys, while the negative values shown in blue are ridge lines. Note the apparent valley-rotation inside the Villany Hills. Inset shows cross-section across the Central Creek (also see Figure 2c). The black rectangles indicate the break points.

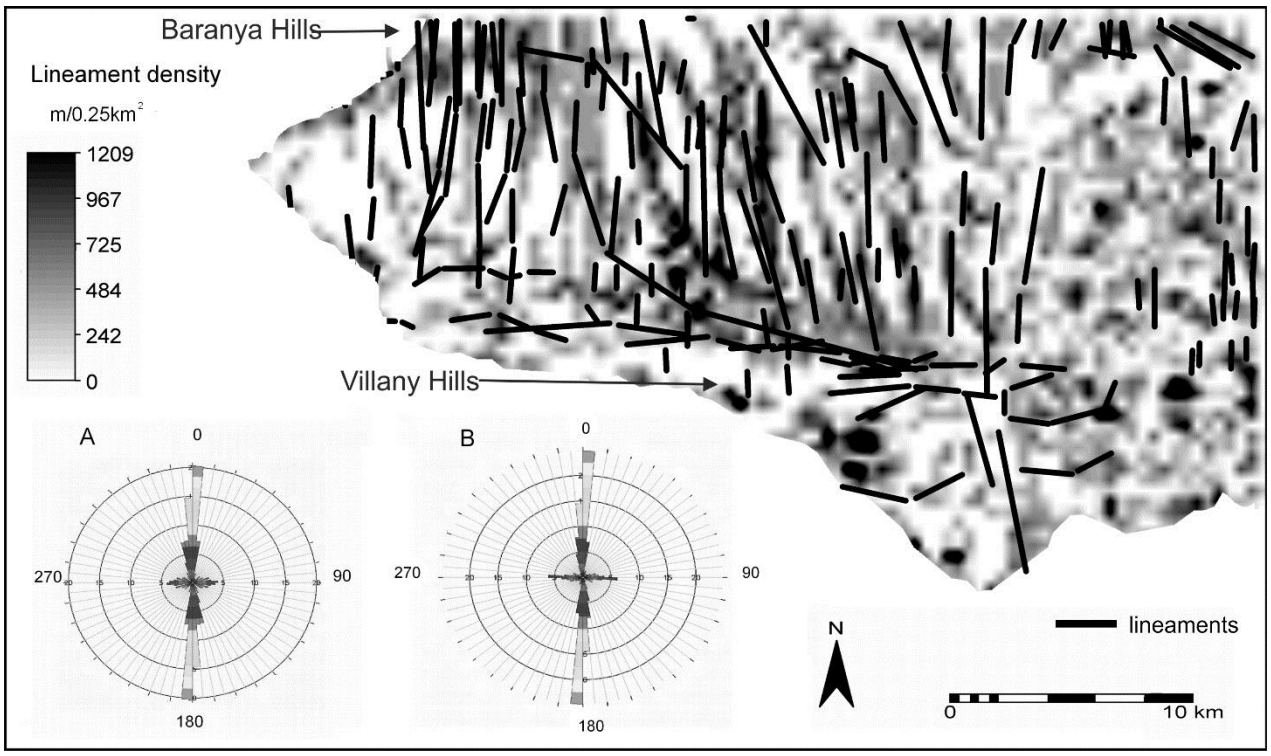

Figure 7. Lineament density map of the study area. Greyscale shading in the background shows the lineament density for the original lineament map in a 500 x 500 m grid. Lineament density is given in units of total length in metre per square kilometre (m/0.25km^2). Inset (A) The direction distribution rose diagram of lineaments. Inset (B) The direction-length distribution of lineaments.

It is apparent that the major N-S running valleys in the Baranya Hills are V-shaped as indicated by the high profile curvature values and show asymmetry in the elevation cross section (Fig. 6, 1. cross-section). It is more interesting that the short N-S running valleys in the Villany Hills have flat bottoms, while the other set of long E-W valleys have V-shaped valley lines irrespective to lithological boundaries. The most interesting is, however, the apparent counter-clockwise rotation of the long ENE-WSW V-shaped valleys (with black colour) in the Villany Hills (Fig. 6).

4.1.3 Lineaments

The digitized lineaments in the Baranya Hills are long and linear, and they have N-S orientation in the west and NNW-SSE in the east. In the Baranya Hills morphological lineaments are concentrated along the equidistantly placed N-S and NNW-SSE running zones, while the Karasica sub-area has a characteristic random spotty pattern in the lineament density map (Fig. 7). Lineaments in the Villany Hills seem to be shorter and more segmented indicating a complex evolution history. The orientation of these lineaments is N-S or E-W, slightly different from those in the Baranya Hills. The lineaments of Villany Hills in the north hit the major NE-SW oriented thrust faults at an about 30 degree angle (Figs. 4c, 7). A narrow high lineament density zone is found with short lineaments at the southern steep slopes of the Villany Hills (Fig. 7).

This pattern highlights the areas of most intensive surface roughness that might be associated with the most fractured Mesozoic bedrock (Fig. 1a, 7). Both frequency-, and length-based orientation distribution rose diagram indicates N-S predominant direction for the total area (Fig. 7 inset a, b).

4.1.4 Digital drainage network analysis

Drainage segment orientation is shown in the rose diagram in figure 8. The NNE-SSW and the NW-SE petals are the longest due to the numerous parallel valleys in the Baranya Hills and Karasica area. The configuration of drainage pattern is quite variable in the total area owing to the complex morphotectonic history. In the Baranya Hills the channels are rather long and parallel to each other, while they are short and rectangular in the Villany Hills (Fig. 8). The drainage density appears to decrease to the west on the south flank of Villany Hills (Fig. 8). Tributaries along the NNW-SSE and N-S trending drainage lines are abundant in the northern Baranya Hills as opposed to the southern region (Fig. 8). Watershed-divides can be identified in the Baranya Hills and in the Villany Hills separating the otherwise continuously aligning

valleys on both sides (see circles along the watershed ridge line in Fig. 8) which indicates relative chronology between the uplift and the drainage network evolution.

Some drainage captures are also revealed in the northern flank of the Villany Hills where the original flow direction is sometimes deviated with more than 70-80°. The map indicates the permanent streams collecting water from the Baranya Hills and Villány Hills and carrying it to the major rivers such as Danube and Drava (Fig. 8).

4.2 Verification of digital terrain analysis

In order to verify the above morphometric and morphotectonic findings, structural data were collected at 12 sites (see Fig. 9a). Seven structural phases were determined from Cretaceous period onward to date by classifying stress fields. The youngest structural phase is characterized by NE–SW compression and perpendicular extension (see Fig. 9a). NNW-SSE to NW-SE trending dextral and NE-SW trending sinistral strike-slip faults are the most prominent elements in this phase (Fig. 9a, sites 2,4,5,6,7,11) but NE-SW trending oblique normal faults are also present (Fig. 9a sites 6,7). This phase represents the youngest one (neotectonic phase?) in the area based on stress-field classification.

This phase was observable in Late Miocene sediments as well (Fig. 9a site 11). The orientation of fault planes is sub-parallel with the manually digitised lineaments (Figs. 7, 9a). The NW–SE trending lineaments are parallel to dextral strike slip faults while the ENE–WSW trending ones have same direction with left lateral strike slip zones of the youngest phase (Fig. 9a). This may indicate the tectonic influence of the youngest phase on the evolution of valleys, ridges, and slope-breaks.

Finally, in addition to field observation, stress field models and archive geological mapping data, 2D NNW–SSE trending interpreted seismic profiles north of the Villany Hills depicting the sub-surface structures of the northern foreland of the Villany Hills and Baranya Hills were also compared to the results of systematic terrain modelling (Figs. 1a,10). The topographic cross-section illustrates the subsurface structures associated with topographic changes identified by the DTA.

Small depressions can be found in front of the thrust faults of the Villany Hills (Fig. 10).

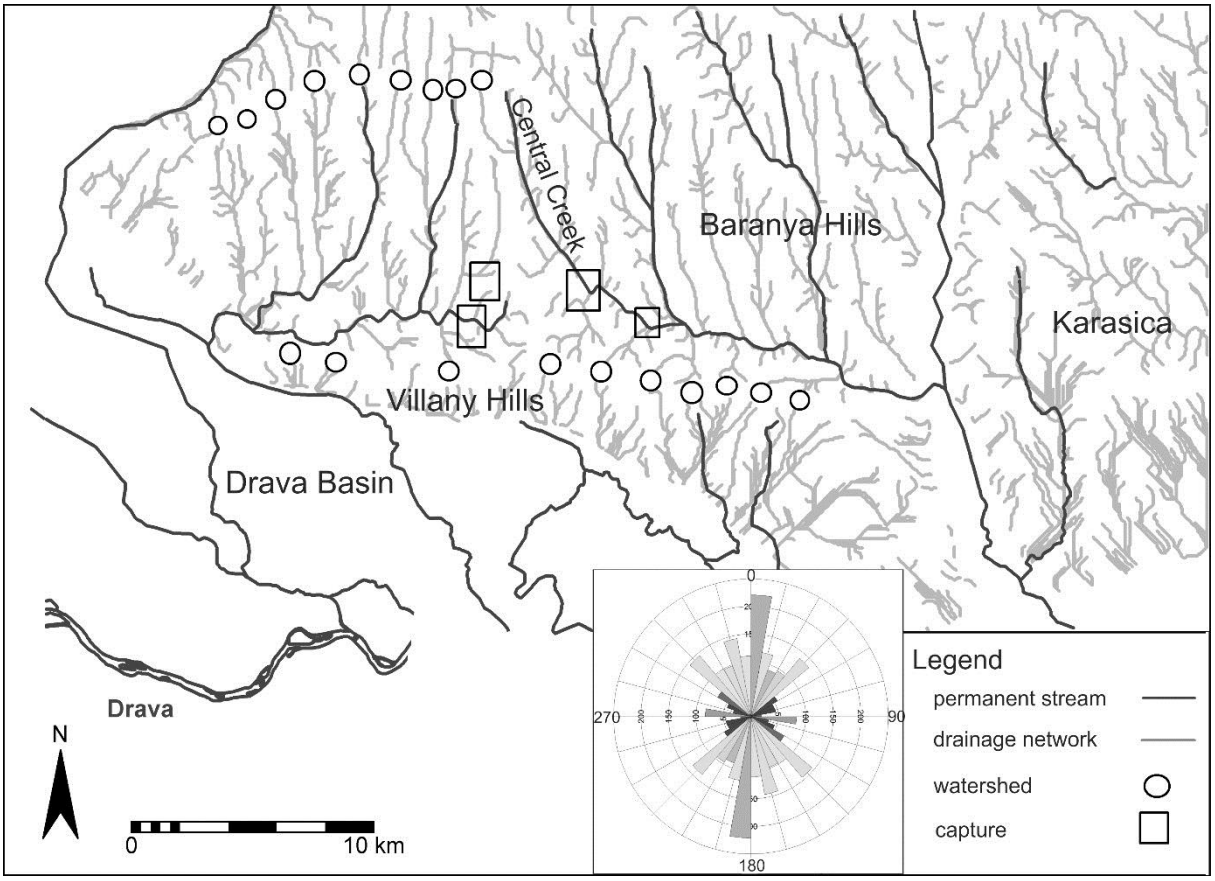

Figure 8. The digital drainage network of the study area. Permanent streams are also shown. Watershed divide and morphological captures are emphasised with light circles and boxes, respectively. Inset: Direction frequency rose diagram of drainage network.

Some slope-breaks can also be seen between the Villany Hills and the Baranya Hills just above some blind faults affecting Late Miocene sediments (Fig. 10). The bordering transpressional faults of the Baranya Hills coincidence with slope-breaks and abrupt topographic changes in north and south as well. This is the area in the Baranya Hills where the relief and slope values are the highest along with lineament density (Figs.3a,b,7). In the NW part of the cross-section which is out of the study area the Mecsekalja Fault zone can be seen with south vergent reverse fault which result in dissected topographic high (Fig. 10).

5. DISCUSSION

The extensive field measurements revealed that the youngest structural phase of the studied area is NE-SW compression starting from Latest Miocene-Pliocene. Recent stress field determination based on borehole breakout and focal mechanism along with structural field measurements were consistent in identifying a stress field with NE–SW compression during the Pliocene and Pleistocene and even Holocene (Bada et al., 2007; Grenerczy & Bada, 2005; Petrik, 2009). The development of the digitally identified morphological features is likely to be associated with the youngest NE-SW compressional, transpressional stress field. Orientations of observed joints and faults belonging to this stress field are mostly parallel to the main morphological features and lineaments (Fig. 9). Subsurface structures and surface topography also show strong correlation with topographic heights above thrust faults and depressions in front of thrust faults (Fig. 10). The digital terrain analysis also revealed that areas with uniform aspect values and high slope angles coincide well with map-scale thrust fault lines especially in the Villány-Hills (Fig. 4c). It is more likely for these thrust lines to anticipate the evolution of NE-SW oriented valleys inside the Villány Hills.

The digital terrain analysis, including cross-sections with strong asymmetry and areas of uniform aspect and slope conditions show that a major E–W oriented morphological lineament may be located at the southern edge of the Villany Hills. Significant break points on classified slope map and profile curvature map are located parallel to the E–W oriented southern flanks of the Villany Hills and to this presumed major lineament (Figs 3c, 6). Further verification of our findings are the hydrogeological evidences which prove that karstic ground flows from the Villany Hills are blocked underground at the southern edge of the hills (Majoros, 2007). This morphological lineament is presumed to be identical to a significant fault (Fig. 9a). The sense of movement along this fault is sinistral strike-slip with reverse components corresponding to the youngest phase (Fig. 9a). The observed CCW valley rotation from east to west and the en-echelon arrangement of NE-SW oriented valley in the Villany Hills also support the sinistral strike-slip tectonics (Fig. 9a). The valley rotation in the Villany Hills is apparent in the classified profile curvature map and shaded relief model (Figs. 6,9a). The orientation of short valleys in the Villany Hills differs with 15–20° from those in the northern Baranya Hills which also indicates the rotation between these two sub-areas (Fig. 4c). Accordingly, E-W sinistral strike-slip faults bound the Villany Hills in the north and in the south corresponding to the NE-SW compressional stress field (Fig. 9a). The morphological features of the Villany Hills are similar and can be explained the best by the en-echelon crestal grabens model of (Burbank & Anderson, 2001) (Fig. 9b).

A high density lineament zone found in the Villany Hills along the border with the Baranya Hills (Fig. 7) in the north refers to an intensive dissection due to asymmetric uplifting of the Villany Hills. During tectonic movement inside the transpressional sinistral fault zone the Villany Hills are being uplifted which corresponds to GPS measurements in the hilly regions of the Pannonian Basin and the recent stress field (Csontos et al., 2002; Grenerczy & Bada, 2005; Petrik, 2011; Wórum, 1999). Uplifting of the Villany Hills is further suggested by a relatively young (Quaternary?) watershed ridge line identified during drainage network analysis (Fig. 8). The drainage network incised into Pliocene-Quaternary sediments north of the Villany Hills. Drainage network captures identified by our study (Fig. 8) developed along the northern border of the Villany Hills can also be explained by the sinistral strike-slip fault.
The highest relief and slope values in the Villany Hills (Fig. 3a,c) also suggest the uplift and its effect on fluvial incision.

In the Baranya Hills the subparallel N-S and NNW-SSE oriented valleys shown by rose diagrams and their geometrical arrangement indicate dextral shear (Fig. 9a) corresponding to the NE-SW youngest compression (Figs. 7,9a). In the eastern part of the Baranya Hills the N-S oriented short subsidiary valleys (Fig. 9a with orange colour) show left-stepping en-echelon arrangement which corresponds to dextral shear along the main NNW-SSE oriented longer valleys (Fig. 9a with white colour).

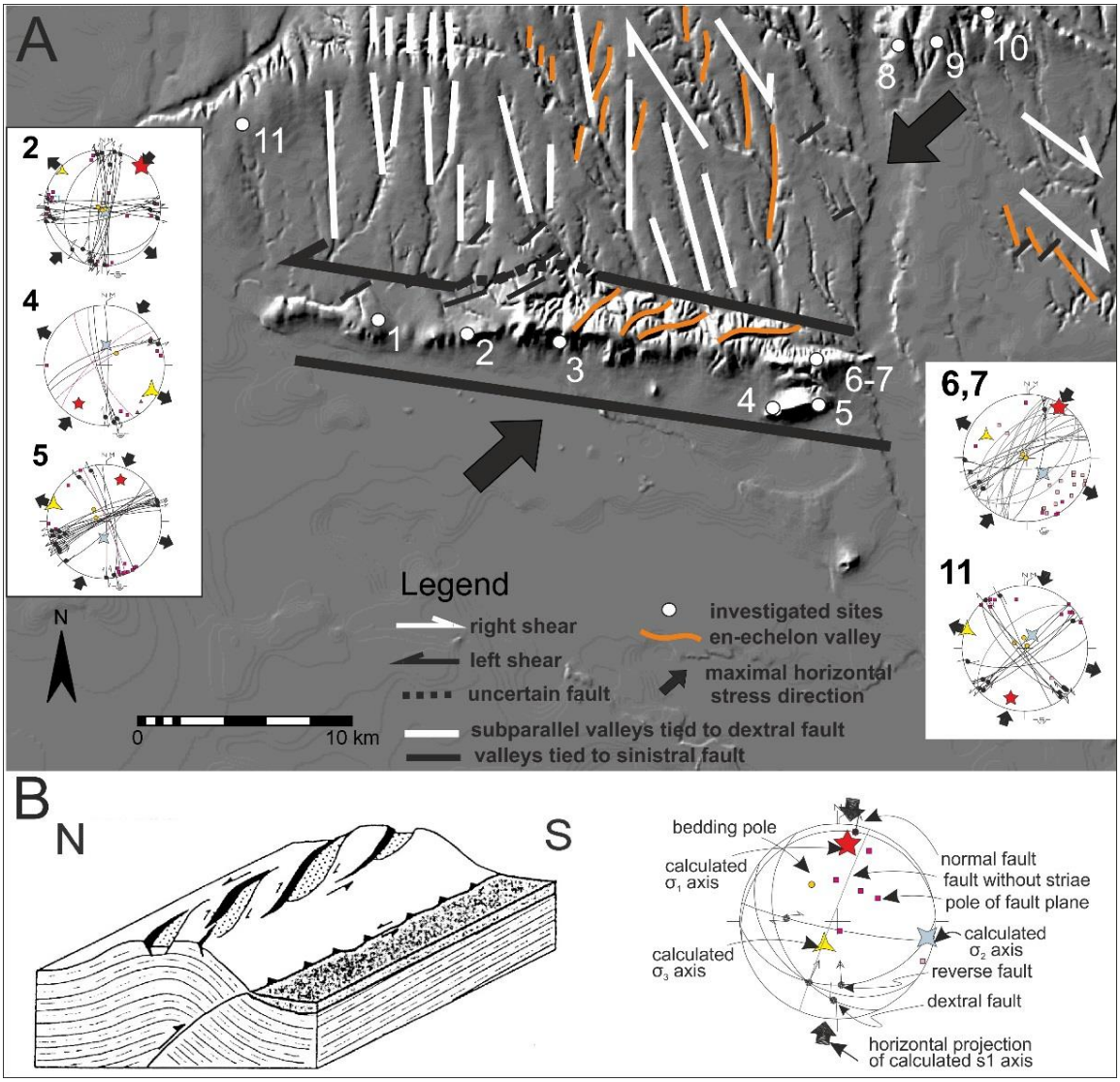

Figure 9a. The study area with the tectonic interpretation of morphological features and some typical stress fields of the youngest structural phase. Figure 9b. The morphotectonic model of the Villány Hills based on Burbank & Anderson's model (2001).

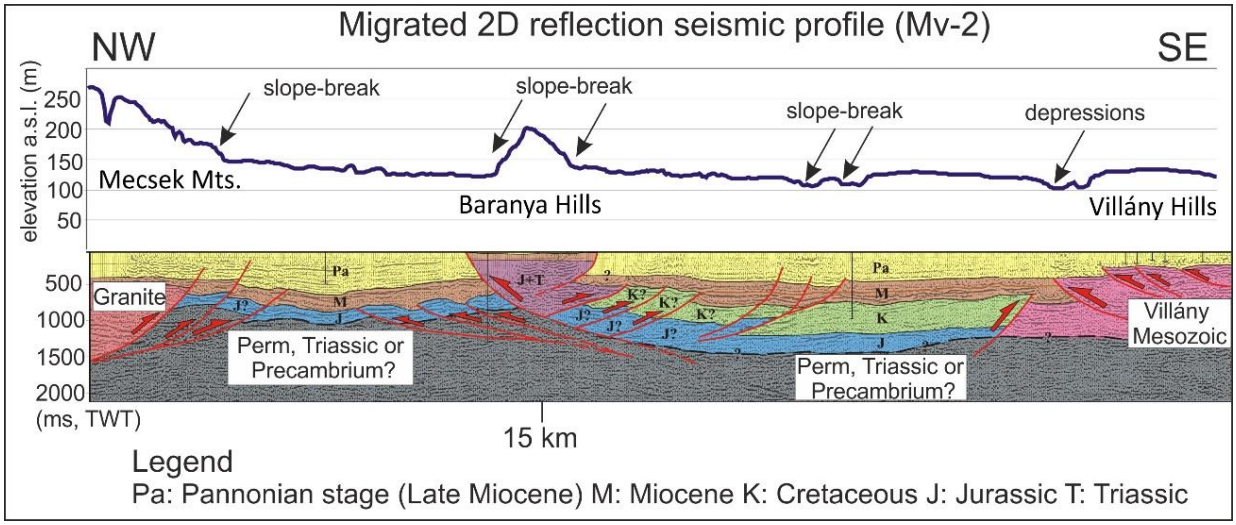

Figure 10. Topographic cross-section along MV-2 seismic profile (The position of Mv-2 section is indicated on Figure 1a.) Blue line represent the surface topography and derives from DEM. Arrows indicate slope-breaks. The seismic interpretation was performed by Wórum (1999)

In case of long subparallel valleys, we cannot exclude the role of wind erosion as an acting force in their development because some wind-blown sand occurrences were described in northern part of the Baranya Hills (Jámbor, 1967). The age of wind-blown sands is late Pleistocene and their source area can be found in the Mecsek Mts to the north (Jámbor, 1967). Sebe et al., (2008) argued that most of the NNW-SSE oriented valleys south of the Mecsek Mts. might have evolved by wind erosion and they used to be blow-outs in late Pleistocene-Holocene.

Nevertheless, our findings point out that based on purely their orientation they might have also evolved by tectonic control because the faults of the youngest structural phase are perfectly parallel to these valleys (Fig. 9a). In addition, the asymmetry in valley profiles west and east in the Baranya Hills as well as the change in their orientation and zig-zagged shape valleys are hardly explained only by wind-erosion. Such a short distance why the orientation of wind would change by 20-40°. Deviation in wind direction was identified in the Transdanubian area but at a larger scale (Fodor et al., 2005).

The uplifting of the Baranya Hills in the north is suggested by the drainage network analysis because dry valleys south from the E-W oriented watershed divide developed at the hinge zone of the hills (Fig. 8). The uplift of the Baranya Hills thus should be younger than the evolution of drainage lines. Baranya Hills is interpreted as inversion pop-up structure by (Wórum, 1999).

E-W oriented cross sections in the Baranya Hills reveal asymmetry in slope angles and elevations between N-S oriented valley-sides (Fig. 2c). This might be a consequence of different tilting of blocks due to the uplifting of the Villany Hills and contemporaneous subsidence of Drava Basin during Late Miocene, Pliocene period (Csontos et al., 2002).

6. CONCLUSIONS

This study has shown the efficiency of systematic digital terrain modelling in morphotectonic analysis. Analysis proceeded from simple univariate analysis of elevation and its derivatives to the more complex bivariate stereonet analyses, digital drainage network analysis and lineament pattern analysis. The applied method uses differential geometry to describe geometric properties of the digital elevation surface and applies digital image processing in each step to enhance and statistically describe terrain models.

The shaded relief models, the classified slope aspect and profile curvature maps, the drainage network map combined with tectonic lines and structural field data yielded essential information on morphotectonics in the present study.

Digitally identified and characterised morphotectonic features were verified by actual detailed field observation of rock fractures along major lineaments. Direct field data provided an unexpected good correspondence with morphotectonic features thereby confirming the appropriateness of the method. Moreover, interpreted 2D seismic profiles showed a convincing match with terrain features such as slope-breaks and asymmetric valleys identified by aspect, slope, curvature, and digital cross-section models (Fig. 10). Fracture lines obtained from previous geological studies, mapping and modelling provided a further independent source of digital terrain model verification. Finally, paleo-stress field models provided considerable explanatory power for the concise interpretation of the observed lineament and terrain feature patterns such as lineament statistics, drainage network characteristics and valley rotation.

Specifically, a significant tectonic fault is presumed at the southern edge of the Villany Hills, the sense of movement is sinistral strike-slip combined with reverse components corresponding to the youngest NE-SW compressional phase and our present morphotectonic findings.

The Villany Hills is a currently uplifting area located inside a major sinistral strike-slip zone. On the crest of the hills many en-echelon ENE-WSW to NE-SW trending deeply incised valleys were identified which evolved as a result of sinistral shear. The location of valleys might have been anticipated by thrust lines whose orientation coincide with them. The orientation of valleys is changing from ENE-WSW to NE-SW from east to the west which can be tied to the major sinistral shear bounding the Villany Hills in the north and in the south. The valley rotation in the Villany Hills is obvious in the classified profile curvature map and in the shaded relief map. Some N-S oriented short valleys were also identified inside the Villany Hills whose orientation deviates from the subparallel longer valleys found in the Baranya Hills. They used to be continuous valleys revealed by drainage lines but the uplift of the Villány Hills and the development of sinistral shear zone changed the orientation. The Villany Hills can be best interpreted by an en-echelon cestral graben model firstly described by Burbank & Anderson (2001).

In the Baranya Hills the 5-15 km long subparallel lineaments (valleys) are changing their

orientation. In the west the N-S direction is prevailing while east from the Central Creek the NNW-SSE orientation become predominant. The subparallel lineaments and their arrangement is excellently fitted in with the youngest structural phase and they can be interpreted as dextral shear zones. The N-S subsidiary short valleys show left stepping en-echelon arrangement which also proves the dextral shear along the N-S longer valleys. However, the wind-erosion in their evolution cannot be excluded and perhaps both of them might have contributed to their evolution.

Acknowledgment

We thank Dr. László Fodor and Prof. Dr. Géza Császár for providing useful information in connection with structural geology and paleogeography of the studied area. We also thank the Norwegian-OTKA Found NNF 78876 Grant help. We also thank the support of the OTKA Fund SNN 118101 Grant help. This paper reports on the research at the GEM-RG Geochemistry, Modelling and Decisions Research Group.

REFERENCES

Bada, G., Dövényi, P., Horváth, F., Szafián, P. & Windhoffer, G., 2007. *Present-day stress field in the Pannonian Basin and the surrounding Alpine-Carpathian-Dianric orogens.* Bulletin of the Hung.Geol.Soc., 137, 327–359. (in Hungarian)

Benkovics, L., 1997. *Etude structuale et géodynamique des Monts Buda, Mecsek et Villány (Hongrie)*. PhD Thesis. L'Universite des Sciences et Technologies de Lille, France, 1–230 (in French)

Burbank, D.W. & Anderson, R.S., 2001. *Tectonic geomorphology*. Wiley, Malden, USA, 1–287.

Byrd, J.O.D., Smith, R.B. & Geissman, J.W., 1994. *The Teton fault, Wyoming: neotectonics, and mechanisms of deformation*. J.Geophys. Res., 99, 20095–20122.

Chorowicz, J., Kim, J., Manoussis, S., Rudant, J., Foin, P. & Veillet, I., 1999. *A new technique for recognition of geological and geomorphological patterns in digital terrain models.* Remote Sens. Environ., 29, 229–239.

Collet, B., Taud, H., Parrot, J.F., Bonavia, F. & Chorowicz, J., 2000. *A new kinematic approach for the Danakil block using a Digital Elevation Model representation.* Tectonophysics, 316, 343–357.

Cotilla, M.O., Córdoba, D. & Herraiz, M., 2007. *A morphotectonic study of the Central System, Iberian Peninsula.* Russian Geology and Geophysics, 48, 378–387.

Császár, G., 2002. *Urgon formations in Hungary with special reference to the Eastern Alps, the Western Carpathians and the Apuseni Mountains.* Geological Institute of Hungary, Budapest, Hungary, 1–209.

Csontos, L., Márton, E., Wórum, G. & Benkovics, L., 2002. *Geodynamics of SW-Pannonian inselbergs (Mecsek and Villány Mts. SW Hungary): Inferences from a complex structural analysis.* EGU Stephan Mueller Special Publication Series, 3, 227–245.

Douglas, D. H., 1986. *Experiments to Locate Ridges and Channels to Create a New Type of Digital Elevation Models.* Cartographica, 23, 29–61.

Drury, S.A., 1987. *Image Interpretation in Geology*. Allen and Unwin, London, UK, 1–279.

Evans, I.S., 1972. *General geomorphometry, derivatives of altitude, and descriptive statistics*. In: Chorley, R.J. (ed.) Spatial Analysis in Geomorphology, Methuen, London, UK, 17–90.

Evans, I.S., 1980. *An integrated system for terrain analysis for slope mapping*. Z. Geomorphology, 36, 274–295.

Florinsky, I.V., 1998. *Combined analysis of digital terrain models and remotely sensed data in landscape investigations.* Prog. Phys. Geogr.,22, 33–60.

Fodor, L., Bada, G., Csillag, G., Horváth, E., Ruszkiczay-Rüdiger, Zs. & Síkhegyi F., 2005. *New data on neotectonic structures and morphotectonics of the western and central Pannonian Basin*. Spec. Issue of Hung.Geol.Inst., 204, 35-44.

Frisch, W., 1997. *Tectonic Geomorphology*. In: Frisch, W., (ed.) Proceeding of the Fourth Int. Conf. on Geomorphology; Z. Geomorphology N. F., Supplementary Band, Germany, 118.

Garbrecht, J. & Martz, L.W., 1999. *TOPAZ: An Automated Digital Landscape Analysis Tool For Topographic Evaluation, Drainage Identification, Watershed Segmentation and Subcatchment Parametrisation: TOPAZ Overview*. U.S. Department of Agriculture, Agricultural Research Service: Washington, DC, USA, 1–24.

Gillespie, A.R., 1980. *Digital techniques of image enhancement*, In: Siegal, B.S. & Gillespie, A.R. (eds.) Remote Sensing in Geology Wiley, USA,1980; 139–226.

Goldsworthy, M. & Jackson, J., 2000. *Active Normal Fault Evolution in Greece Revealed by Geomorphology and Drainage Patterns.* Geological Society, Special Publication, 157, 967–981.

Grenerczy, Gy. & Bada, G., 2005. *GPS baseline length changes and their tectonic interpretation in the Pannonian Basin.* Geophysical Research Abstracts, 7, No. 04808

Grohmann, C.H., Riccomini, C. & Alves, F.M., 2007. *SRTM-based morphotectonic analysis of the Poços de Caldas Alkaline Massif, southeastern Brazil.* Computers & Geosciences, 33, 10–19.

Gyalog, L. & Síkhegyi, F., 2010. *1:100.000 Geological map of Hungary*. In: Gyalog, L. & Síkhegyi, F.

(eds.) Geological map of Hungary CD-ROM*;* Geological Institute of Hungary, Budapest, Hungary.

Hobbs, W.H., 1912. *Earth Features and their Meaning*. Macmillian Co., New York.

Jámbor Á., 1967. *Pleistozäne Deflationserscheinungen im südwestlichen Teil des Mecsek-Gebirges*. Acta Universitatis Szegediensis, Acta Mineralogica Petrographica 18,1,13-22. (in German)

Jordan, G., 2003. *Morphometric analysis and tectonic interpretation of digital terrain data: a case study.* Earth Surf. Process. Landforms, 28, 807–822.

Jordan, G., 2007. *Digital terrain analysis in a GIS enviroment. Concepts and development*. In: Peckham, R.J. & Jordan, G. (eds.) Digital terrain modelling, Development and applications in a policy support environment*;* Springer Verlag, Berlin, Germany, 2–39.

Jordan, G. & Csillag, G., 2003. *A GIS framework for morphotectonic analysis – a case study.* Proceedings of Fourth European Congress on Regional Geoscientific Cartography and Information Systems, Bologna, Italy, Proceedings, 2, 516 – 519.

Jordan, G., Meijninger, B.M.I., Hinsbergen, D.J.J., Meulenkamp, J.E. & Dijk, P.M., 2005. *Extraction of morphotectonic features from DEMs: Development and applications for study areas in Hungary and NW Greece*. International Journal of Applied Earth Observation and Geoinformation, 7, 163–182.

Keller, E.A. & Pinter, N., 1996. *Active Tectonics: Earthquakes, Uplift and Landforms*. Prentice Hall, New Jersey, USA, 1–362.

Kleb, B., 1973. *Geologie des Pannons im Mecsek.* Annales Rep. Hung. Geol. Inst., 53, 743–943. (in German)

Majoros, Gy., 2007. *The geological and hydrogeological overview of the Villány Hills.* Mecsekérc Zrt., Pécs, Hungary, 1–22. (in Hungarian)

Martz, L.W. & Garbrecht, J., 1992. *Numerical definition of drainage networks and subcatchment areas from digital elevation models.* Computers & Geosciences, 18, 747–761.

Nagy, E. & Nagy, I., 1976. *Triassic formations in the Villany Hills.* Geologica Hungarica, Series Geologica, 17, 113–227 (in Hungarian)

Onorati, G., Poscolieri, M., Ventura, R., Chiarini, V. & Crucilla, U., 1992. *The digital elevation model of Italy for geomorphology and structural geology*. Catena, Italy, 19, 147–178.

Parul, N., Joshi, M.D.M. & Chamyal, L.S., 2013. *Morphotectonic segmentation and spatial variability of neotectonic activity along the Narmada–Son Fault, Western India: Remote sensing and GIS analysis.* Geomorphology, 180–181, 292–306.

Petrik, A., 2009. *Interpretation of the results of microtectonic measurements performed with respect to Mesozoic formations of the Villány Hills, Hungary.* Bulletin of the Hung.Geol.Soc., 139, 217–236. (in Hungarian)

Petrik, A., 2011. *Microtectonic measurements and interpretation of the Mesozoic formations in the Villány Hills and Görcsöny-Máriakéménd Ridge, Hungary*. Central European Geology, 53, 21–42.

Peucker, T.K. & Douglas, D.H., 1975. *Detection of surface-specific points by local parallel processing of discrete terrain elevation data.* Comput. Graphics Image Process., 4, 375–387.

Prost, G.L., 1994. *Remote sensing for geologists*. Gordon and Breach Science Publischers, Amsterdam, Netherlands, 1–623.

Rakusz, Gy. & Strausz, L., 1953. *The geology of the Villány-Hills*. The year book of the Geological Institute of Hungary, Budapest, Hungary, 41, 3–27.

Ramsay, J.G. & Huber, M.L., 1987. *The Techniques of Modern Structural Geology*. *Vol. 2. Folds and Fractures*. Academic Press, London, UK, 1–697.

Ruibo, W. & Weiming, C.H., 2009. *Extraction of Tectonic Faults of Longmen Mountain Based on DEM.* 2nd International Congress on Image and Signal Processing, CISP '09. Tianjin, China, 4.

Salvi, S., 1995. *Analysis and interpretation of Landsat synthetic stereo pair for the detection of active fault zones in the Abruzzi Region (Central Italy).* Remote Sens. Environ., 53, 153–163.

Sebe, K., Csillag, G. & Konrád, Gy., 2008. *The role of neotectonics in fluvial landscape development in the Western Mecsek Mountains and related foreland basins (SE Transdanubia, Hungary)*. In: Silva, P.G., Audemard, F.A. & Mather, A.E. (eds.) Impact of Active Tectonics and Uplift on Fluvial Landscapes and River Valley Development; Impact of Active Tectonics and Uplift on Fluvial Landscapes and River Valley Development, Geomorphology, 102, 55 – 67.

Siart, C., Bubenzer, O. & Eitel, B., 2009. *Combining digital elevation data (SRTM/ASTER), high resolution satellite imagery (Quickbird) and GIS for geomorphological mapping: A multi-component case study on Mediterranean karst in Central Crete.* Geomorphology, 112, 106–121.

Simpson, D.W. & Anders, M.H., 1992. *Tectonics and topography of the Western United States an application of digital mapping.* GSA Today, 2, 118–121.

Takahashi, S., Ikeda, T., Shinagawa, Y., Kunii, T.L. & Ueda, M., 1995. *Algorithms for extracting correct critical points and constructing topological graphs from discrete geographical elevation data.* The International Journal of the Eurographics Association, 14, 181–192.

Vadász, E., 1935. *Geologie des Mecsek Gebirges*. Publ. Hung. R. Inst. Geol., Budapest, Hungary, 73–82 (in German).

Whipple, K. X. & Tucker, G. E., 1999. *Dynamics of the stream power river incision model: Implications for height limits of mountain ranges,*

landscape response timescales and research needs, J. Geophys. Res., 104, 661 –674.

Wórum, G., 1999. *The structural evolution of the Mecsek-Villány Region based on seismic section analysis.* MSc thesis, ELTE Geophysical Dept., Budapest, Hungary (in Hungarian)

Wu, L., Wang, N., Han, M., Ren, F. & Chen, Y., 1993. *Methods and applications of a geomorphological GIS:a case study in the Ordos region of China*. ISPRS Journal of Photogrammetry and Remote Sensing, 48, 38–45.

Received at: 26.07. 2016
Revised at: 17. 10. 2016
Accepted for publication at: 13. 11. 2016
Published online at: 16. 11. 2016